

NACA TN 3758 16097

006625



TECH LIBRARY KAFB, NM

NATIONAL ADVISORY COMMITTEE FOR AERONAUTICS

TECHNICAL NOTE 3758

INTERACTION OF BEARING AND TENSILE LOADS
ON CREEP PROPERTIES OF JOINTS

By E. G. Bodine, R. L. Carlson, and G. K. Manning

Battelle Memorial Institute



Washington

October 1956

AFMTC
TECHNICAL



TECHNICAL NOTE 3758

INTERACTION OF BEARING AND TENSILE LOADS

ON CREEP PROPERTIES OF JOINTS

By E. G. Bodine, R. L. Carlson, and G. K. Manning

SUMMARY

The objective of this investigation was to study the interaction of bearing and tensile loads on the creep behavior of joints. To achieve this objective, a specimen was designed which possessed some of the general features of pin and rivet joint connections. An apparatus was constructed to apply both bearing and tensile loads to the joint model.

Measurement of deformation was accomplished by the use of a photo-grid printed on the joint model. Analysis of the deformation patterns indicates that the form of the strain-history curves at some points in the simulated joint is similar to that of the strain-history curves for uniaxial tensile creep tests. Further, there appears to exist a steady-state period during which certain creep strain rates remain constant. This may imply that the stress distribution during that period is also constant over part of the specimen.

For the tested specimens, hole elongation due to combined bearing and tensile loading was composed of an elongation due to the total tension plus an elongation due to bearing. When the bearing load was not excessive, the elongation due to bearing appeared to be transient, and additional hole elongation continued at a rate that was approximately equal to that for a tensile load of the same total magnitude.

The fracture appearance of specimens subjected to tension and of specimens subjected to tension and bearing was similar. The extent of certain fracture zones differed for the two cases, however.

The results of this exploratory study indicate that several features of the deformation behavior may be amenable to a simplified analysis. Before final conclusions can be made, however, more detailed measurements should be made, and additional tests should be conducted.

INTRODUCTION

It has often been observed that the satisfactory design of a structural assembly made up of many elements cannot be achieved simply by using basic material data to predict the behavior of the structure as a whole. One case in which such a correlation has been found difficult is that of loaded composite structures exposed to operating temperatures high enough to cause creep. It has been found (refs. 1 and 2), for example, that the deformation contribution at riveted connections is greater than had been anticipated. The successful design of high-temperature structures that include joints can, therefore, be affected only if proper allowance is made for joint deformation.

One of the objectives of this investigation was to develop a simple joint model that possessed some of the essential features of pin- and rivet-type connections. It was felt that a study of the modes of deformation resulting from various combinations of loading might furnish a basis for simplifying assumptions that would permit the prediction of joint behavior. The specimen which was used as a joint model (fig. 1(a)) allowed the application of both bearing (through a pin) and tensile loads. A limitation of the design is that rivet-head pressures and subsequent sheet friction cannot be represented.

In many sheet riveted connections, the stress distribution present in the vicinity of the rivet hole can approximately be represented as the sum of two stress systems, one due to tension and one due to bearing (applied through a rivet in the hole). The superposition of these two types of stresses should result in a fair approximation to those in the riveted joints of actual structures. The ratio of the loads to one another would depend on the manner of loading, the type of joint, and the number of rivets. It should be possible, however, to simulate many joints simply by varying the ratio of tension to bearing.

During this initial, exploratory study, emphasis was placed on evolving a system for observing and evaluating the deformations due to various load combinations. In addition, it was felt that a complete analysis of the case of tension alone would be necessary for the simplification of the more complicated case of an actual joint connection. Thus, much of the preliminary work was devoted to this case.

This investigation was conducted at Battelle Memorial Institute under the sponsorship and with the financial assistance of the National Advisory Committee for Aeronautics.

EXPERIMENTAL WORK

Specimens

The specimens used for this investigation were cut from a 1/8-inch-thick sheet of 2024-0 aluminum alloy. The loading axis of the specimens was perpendicular to the direction of rolling. Specimen drawings are shown in figure 1. The material was tested in the as-received condition.

To enable measurements of the deformations that took place during the testing to be made, a photogrid was applied to one face of each specimen (see fig. 2). The technique used to apply the photogrid is described in a later section.

Apparatus

The special fixture shown in figure 3 was constructed for applying tensile and bearing loads to specimens of the type shown in figure 1(a). Essentially, the apparatus is a lever-type tensile loading frame with an additional lever to apply a bearing load. Since the lines of action of the two forces are superimposed, the bearing load is applied by a pin and yolk arrangement so that the bearing load remains independent of the tensile load. Both loads remain constant throughout a test.

The electric furnace which enclosed the specimens maintained the test temperature of 400° F to within 8° F on the 15-inch specimen. Near the central 9-inch gage section, the temperature variation was less than 4° F. A Minneapolis-Honeywell proportioning controller was used to control the temperature during tests.

Procedure

The tensile stress-strain diagram at elevated temperature (fig. 4) and the tensile creep curves (fig. 5) of the material were obtained from tests made on the specimen shown in figure 1(b).

For the tests in combined tensile and bearing loading, the specimen shown in figure 1(a) was used. To perform this test, the specimen was placed in the testing machine, and a small tensile load was applied. If a bearing load was to be used, a hardened steel pin 0.495 inch in diameter was placed through the hole in the specimen, and a small bearing load was applied. The furnace was closed, and the specimen was heated to the test temperature (400° F) in about 40 minutes. After an additional 20-minute temperature-stabilization period, the test load was applied. In each combined-loading test, the tensile load was completely

applied before any bearing load was introduced. It is likely that the order of loading will have some effect on the deformations that occur. This would be expected particularly for those cases in which the deformation is small. However, after large creep deformations have taken place, the order of initial loading should become less significant.

After a selected interval, the load was removed, and the specimen was allowed to cool to room temperature. All specimens were tested at 400° F, and test periods ranged from less than 1 minute to over 24 hours.

Measurement of Strain

The photogrid that was applied to the specimen formed squares measuring 0.0500 ± 0.0001 inch and oriented with their sides perpendicular and parallel to the axis of the specimen. After testing, these squares had deformed plastically and their new dimensions were measured. Thus, longitudinal and transverse strains could be obtained.

Measurements were made with a Gaertner micrometer comparator, the smallest reading of which was 0.00005 inch. This implies a sensitivity of 50 microinches. The deviation from the average in four readings for large values of strain (over 10 percent) was never greater than 0.00025 inch, indicating a reproducibility of better than 5 percent. Down to about 1-percent strain, the reproducibility was better than 10 percent.

Application of Photogrid

The face of the specimen which was to receive the photogrid was cleaned first with steel wool and then with pumice powder. The specimen was then placed in a warmed box (about 140° F) and sprayed with a photographic emulsion of the following composition: 4 parts of photoengraver's glue, 23 parts of water, 1 part of ammonium dichromate, and 1/4 part of ammonia water (refs. 3 and 4). For spraying, the above solution was diluted by mixing 1 part of the solution to 3 parts of water and 4 parts of ethyl alcohol. It was not necessary to perform this work under dark-room conditions. Direct exposure to sunlight was, however, avoided. Six thin coats of the diluted emulsion were applied. Approximately 20 minutes of drying time between applications was allowed.

Negatives made from a diamond-ruled glass plate (20 lines to the inch) were placed over the emulsified face of the specimen, and printing was accomplished by exposure to a No. 2 photoflood lamp. The time for exposure was about 16 minutes, and the distance from bulb to plate was about 1 foot. An electric fan kept the specimen cool during exposure. The printed emulsion was developed by washing the specimen in a solution of clothes dye and water for about 5 minutes. After drying, the grid

formed on the specimen was generally impervious to moderate handling and was capable of withstanding exposure to the test temperature of 400° F.

DISCUSSION OF RESULTS

The design of joints subjected to creep can be based either on an allowable amount of deformation or on fracture. The approach in studying joint behavior would differ in each case. If fracture is the only important consideration, a large number of stress-rupture types of tests would yield information for design. However, if allowable deformation is the criterion, a more elaborate analysis involving strain histories is necessary, and fewer but more detailed tests must be performed. Often a more conservative design is necessary than that suggested by fracture data. This investigation was concerned primarily with recording deformation histories.

An important factor that has not been investigated in this exploratory study is the effect of the geometry of the test model. It is expected that the hole diameter-to-width ratio, hole diameter-to-thickness ratio, and hole width-to-thickness ratio will have effects on the deformation patterns. Further tests are needed to evaluate these effects.

Plate Subjected to Tension

When the plate area surrounding a hole is under a sufficiently high tensile stress and at an elevated temperature, creep will occur. Unfortunately, the strains will not be uniform across a section containing the hole because of the stress concentration caused by the presence of the hole. In figure 6, the maximum strains in the test specimen of figure 1(a) are shown after various periods of time had elapsed. The applied stress¹ of 14,000 psi was above the yield point of the material. Strains were measured in the direction of the applied stress along a line perpendicular to the load and passing through the center of the hole (line A-A). Also shown in figure 6 are the theoretical strains that would have occurred had the plate remained elastic (refs. 5 and 6) and the strains due to the initial plastic loading (zero time). Previous work (refs. 7 and 8) on 2024-T3 aluminum-alloy sheet at room temperature has shown that the stress and strain concentration factors near a hole in a very wide plate subjected to plastic loading are given approximately by

¹The term "applied stress" refers to the longitudinal stress across a section of the specimen away from the hole.

$$\sigma C.F. = 1 + 2 \frac{(E_S)_{a, \pi/2}}{(E_S)_\infty}$$

and

$$\epsilon C.F. = 2 + \frac{(E_S)_\infty}{(E_S)_{a, \pi/2}}$$

where

$\sigma C.F.$ stress concentration

$\epsilon C.F.$ strain concentration

$(E_S)_{a, \pi/2}$ secant modulus at point of maximum stress

$(E_S)_\infty$ secant modulus at a point far removed from hole

The concentrations computed from these formulas for the values from figure 6 are:

$$\sigma C.F. = 1.34$$

$$\epsilon C.F. = 7.85$$

Experimentally determined values are:²

$$\sigma C.F. = 1.56$$

$$\epsilon C.F. = 9.13$$

The difference between the calculated and experimental values can probably be attributed to a difference in the geometry and properties of the material used in this study and of that used in reference 7.

It was difficult to observe the rates of strain from figure 6, and figure 7 was therefore prepared. It shows the strains in the direction of the applied stress at various points along line A-A as functions of time. Since the general appearance of these curves is similar to that of uniaxial creep curves, the zones have been labeled "primary," secondary," and "tertiary."

²Although the stresses at the interior are biaxial, they are uniaxial at the free edges of the specimen. For the edges, it is possible to obtain values of stress from the observed strain and the uniaxial stress-strain diagram (fig. 4). This is what has been done to compute the experimental value of stress concentration.

The primary stage is, no doubt, related to the primary stage which would occur for tensile specimens under constant stress. The primary stage in figure 7 is somewhat more complex, however, since the stresses on the fibers are not constant, particularly near the hole. During the primary stage, the stresses are undergoing continuous readjustment. Stresses adjacent to the hole can be expected to decrease or relax, and those away from the hole can be expected to increase slightly.

The existence of approximately constant creep rates for fibers along line A-A (see fig. 6) during the secondary stage has tentatively been taken to imply a fixed or steady-state stress distribution along line A-A. It should be emphasized that, if a steady state does exist, it exists only during the secondary stage. Further, regions above and below line A-A are probably not steady-state regions. It is possible, however, that the steady-state zone may tend to grow. Future additional measurements may reveal this.

Since strain rates decrease away from the hole, lines originally parallel to line A-A would be expected to rotate with respect to A-A. Figure 2, which shows photographs of deformed specimens, indicates the occurrence of such rotation. As indicated above, further detailed analysis of regions adjacent to line A-A should provide more insight into the kinematics of the deformation.

An attempt was made to derive the stresses along line A-A by comparing the creep rates of figure 7 (secondary stage) with creep rates for tensile creep. (Strictly speaking, such a comparison can be made only at the free edges of the specimen.) This attempt was not successful because the secondary creep rates from the tests conducted (see fig. 5) were too low. Further tensile creep tests at higher stress levels should make such a comparison possible.

After sufficient elongation (and corresponding reduction in area) of the fiber at the edge of the hole, the creep rate increased until fracture occurred. It is interesting to note from figure 7 that the entire cross section apparently entered a third stage in rapid succession, even though the strains farther from the hole would not be expected to do so for some time. This can be attributed to a shifting of load from the weakened fibers nearest the hole to those farther away.

The net effect of the strains in the area surrounding the hole was to produce an elongation of the hole in the direction of the applied stress. Figure 8 shows the hole elongation due to various applied stresses and figure 9 shows the hole elongation due to creep. The initial hole elongation (fig. 8) resulted mainly from a small but definite plastic zone adjacent to each side of the hole at the points of maximum stress. As the stress level increased, the plastic zone spread, causing a still greater hole elongation.

The creep elongations of figure 9 had the same general form as that of a uniaxial creep curve. It is interesting to note that the secondary rate of hole elongation was approximately one-half the secondary rate of maximum strain (measured immediately adjacent to the hole) in tests at both 14,000 and 10,000 psi. A comparison was not obtained at 8,000 psi because it was felt that the strains at that stress were too small to be reliably measured by the method that was used. It would be expected that the hole elongation would be a function of some kind of average of the adjacent strains. Analysis of more experimental data is necessary, however, before any definite conclusion can be reached as to what the nature of this relationship may be.

Plate Subjected to Tension and Bearing

Figure 10 shows the strains in test specimens that were subjected to the combined effect of bearing and tension. The total load on each specimen was the same as that applied to the specimens of figure 6. The tension and bearing loads were equal, and the actual load values are indicated in figure 10. Figure 11 shows the strains as functions of time. The form of these curves is similar to that of the curves of figure 7 for tension alone.

Comparing figures 6 and 10, it is seen that the maximum strains in the case of combined loading are higher than those for tension alone. In addition, the strains remain relatively high for a greater distance away from the hole, indicating that a larger area near the hole remains subjected to high tensile stresses.

The rates of strain adjacent to the hole (from figs. 7 and 11) for combined loading are greater than those for tensile loading. Farther away, however, the rates are approximately the same for both types of loading. This again indicates that the effect of bearing is less highly localized. Far away from the hole, the strains can be considered due entirely to the tensile stresses produced by the applied loads.

Intuitively, it would seem that the rate of compressive creep deformation due to the bearing pin for small bearing loads would eventually become stabilized and be small compared with the tensile creep rate. This would occur as a result of a buildup of material in front of the pin. Evidence supporting this tendency is shown in figure 12. Here the variation of rivet hole elongation with time is shown for three cases of combined loading. The dashed lines represent hole elongation for the case of tension alone. In the case of the two lower stresses (8,000 and 10,000 psi) the rate of elongation is approximately the same for combined loading as for tensile loading. Apparently, at 14,000 psi, the specimen fractured before the rate of bearing deformation became small. The ratio

of tensile load³ to bearing load was 2:1 for the 14,000- and 10,000-psi tests and 3:2 for the 8,000-psi test. Even for the high percentage of bearing load in the last case, the principal influence on the rate of hole elongation was the total tensile stress across the section.

Ultimately, it is hoped that the observed features of the deformation behavior may provide a basis for the development of a simplified method of analyzing joint deformation. Joint-deformation analysis may, for example, be simplified if the tensile load acting on section A-A of figure 1(a) is assumed to be a good index of deformation, regardless of the loading combination. For the data presented, the deformations at the outer edges of the specimens were approximately equal when the tensile loads across section A-A were the same. Further, it appeared that hole elongation due to bearing deformation in front of the bearing pin may be transient when the bearing load is not excessive. Continued hole elongation proceeded at a rate that appeared to depend on the tensile load across section A-A.

It should be emphasized that the simplification suggested is to a large extent speculation based on a limited amount of test data. Before any conclusive statements can be made, additional work should be conducted. An analysis of tests at more load levels and at several load ratios would be particularly helpful.

Fracture Appearance

Often, the mode of fracture is indicative of the manner in which fracture initiates and propagates. Figure 2 shows the fracture appearance of a specimen subjected to tension alone and of a specimen subjected to tension and bearing. In each case the tensile load⁴ was the same. The ratio of tension to bearing for the combined loading was 2:1.

There were two distinct modes of fracture associated with each specimen. A form of cup and cone fracture in which the reduction in thickness was of the order of 50 percent occurred in the highly stressed region near the edge of the hole. Away from the hole, an abrupt change to a 45° shear type of fracture began and continued to the outer edges of the specimen. Here, the reduction in thickness was about 10 percent.

In the case of tension alone, the cup and cone appearance extended about 0.15 inch from each side of the hole. In the case of combined

³Tensile load is defined here as the load acting on section A-A of figure 1(a). For bearing alone, as in a single rivet lap joint, the ratio is 1:1. For tension alone, the ratio is 1:0.

⁴Tensile load through section A-A of figure 1(a).

loading, the cup and cone appearance extended about 0.40 inch from the hole. This indicates that the region of high stress is extended by the combined loading. This fact was also deduced earlier from the appearance of the strain patterns adjacent to the hole.

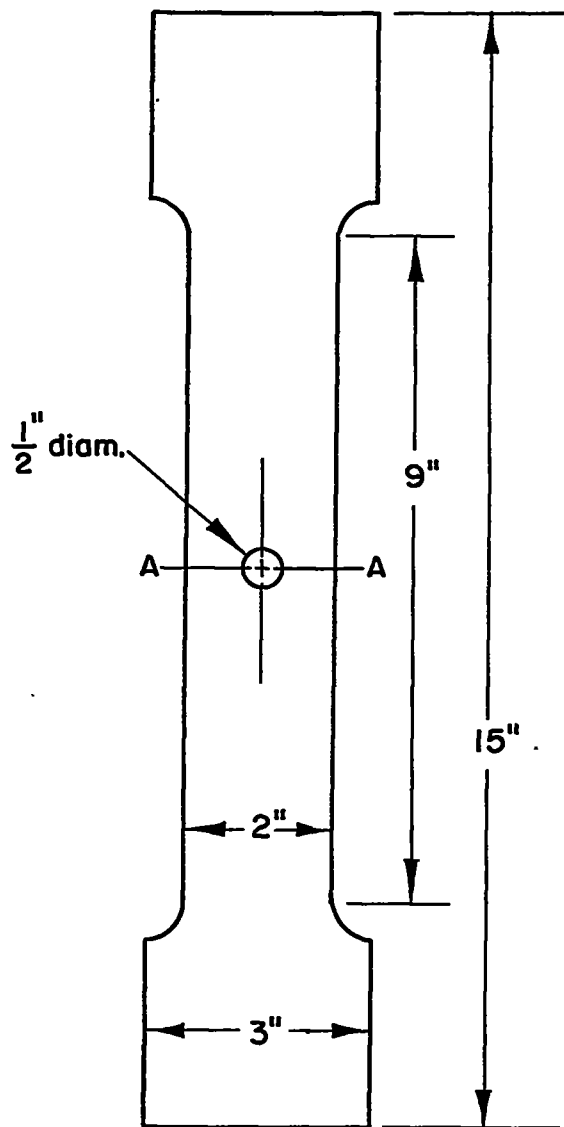
It is not too apparent from figure 2, but only the outer edges of the fractured specimens fit together. A part of this gap could have been contributed by elastic "spring back" in the central portion of the specimen. A greater part of the gap is, however, probably the result of the deformation continuing at the outer edges while the cracks were progressing outward.

It is apparent from the above discussion that fracture in these tests initiated after the ductility of the material adjacent to the hole was exhausted. Subsequent crack propagation then occurred quickly with relatively little local reduction in thickness.

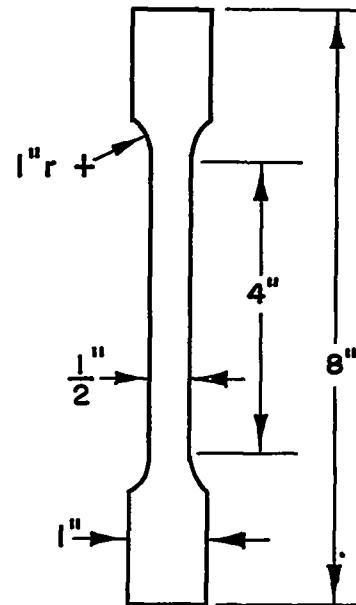
Battelle Memorial Institute,
Columbus, Ohio, January 3, 1955.

REFERENCES

1. Mordfin, Leonard: Creep and Creep-Rupture Characteristics of Some Riveted and Spot-Welded Lap Joints of Aircraft Materials. NACA TN 3412, 1955.
2. Hill, H. N., and Barker, R. S.: Effect of Open Circular Holes on Tensile Strength and Elongation of Sheet Specimens of Some Aluminum Alloys. NACA TN 1974, 1949.
3. Brown, W. F., Jr., and Jones, M. H.: Strain Analysis by the Photogrid Method. The Iron Age, vol. 158, no. 11, Sept. 12, 1946, pp. 50-55.
4. Brewer, Given A., and Glassco, Robert B.: Determination of Strain Distribution by the Photo-Grid Process. Jour. Aero. Sci., vol. 9, no. 1, Nov. 1941, pp. 1-7.
5. Timoshenko, S., and Goodier, J. N.: Theory of Elasticity. Second ed., McGraw-Hill Book Co., Inc., 1951, pp. 78-85.
6. Howland, R. C. J.: On the Stresses in the Neighbourhood of a Circular Hole in a Strip Under Tension. Phil. Trans. Roy. Soc. (London), ser. A, vol. 229, no. 671, Jan. 6, 1930, pp. 49-86.
7. Griffith, George E.: Experimental Investigation of the Effects of Plastic Flow in a Tension Panel With a Circular Hole. NACA TN 1705, 1948.
8. Stowell, Elbridge Z.: Stress and Strain Concentration at a Circular Hole in an Infinite Plate. NACA TN 2073, 1950.



(a) Joint-model specimen.



(b) Tensile test specimen.

Figure 1.- Test specimens.

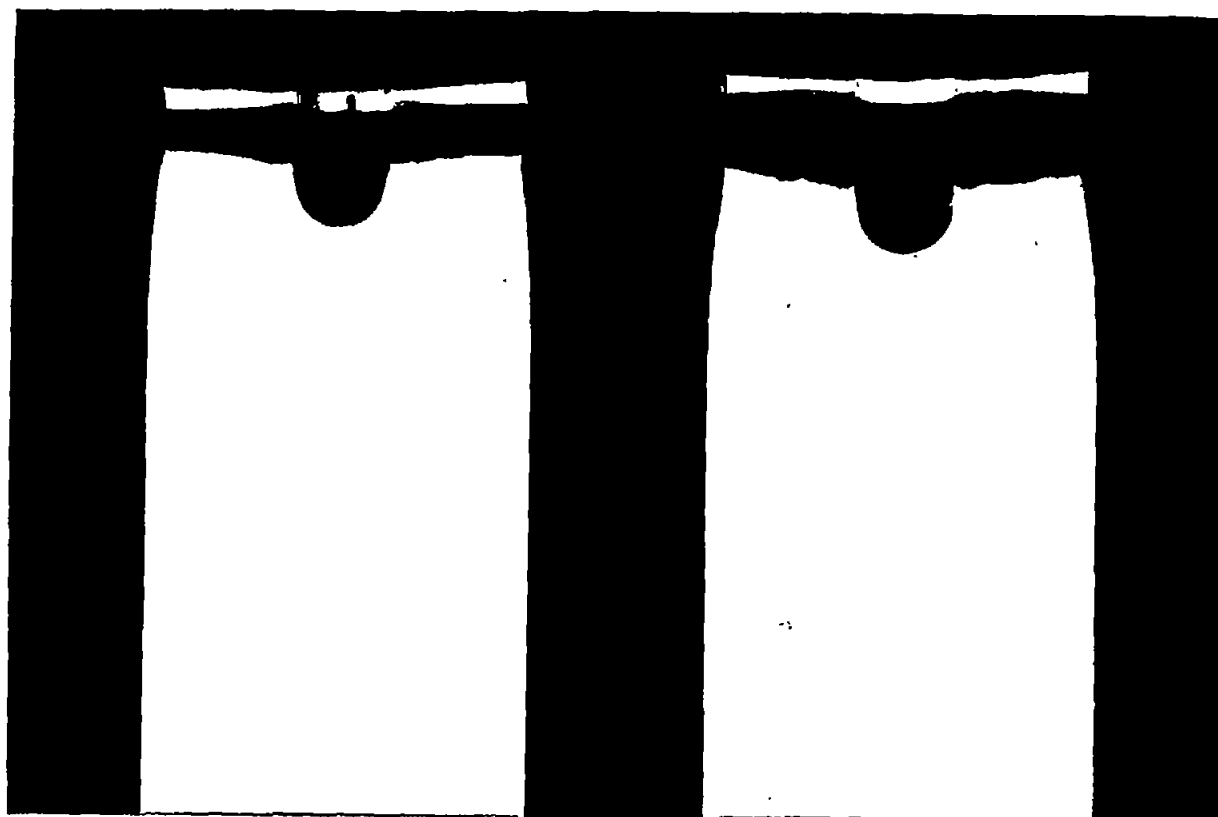


Figure 2.- Fracture of plate with hole. Specimen at left was subjected to tension. Specimen at right was subjected to tension and bearing.

L-93512

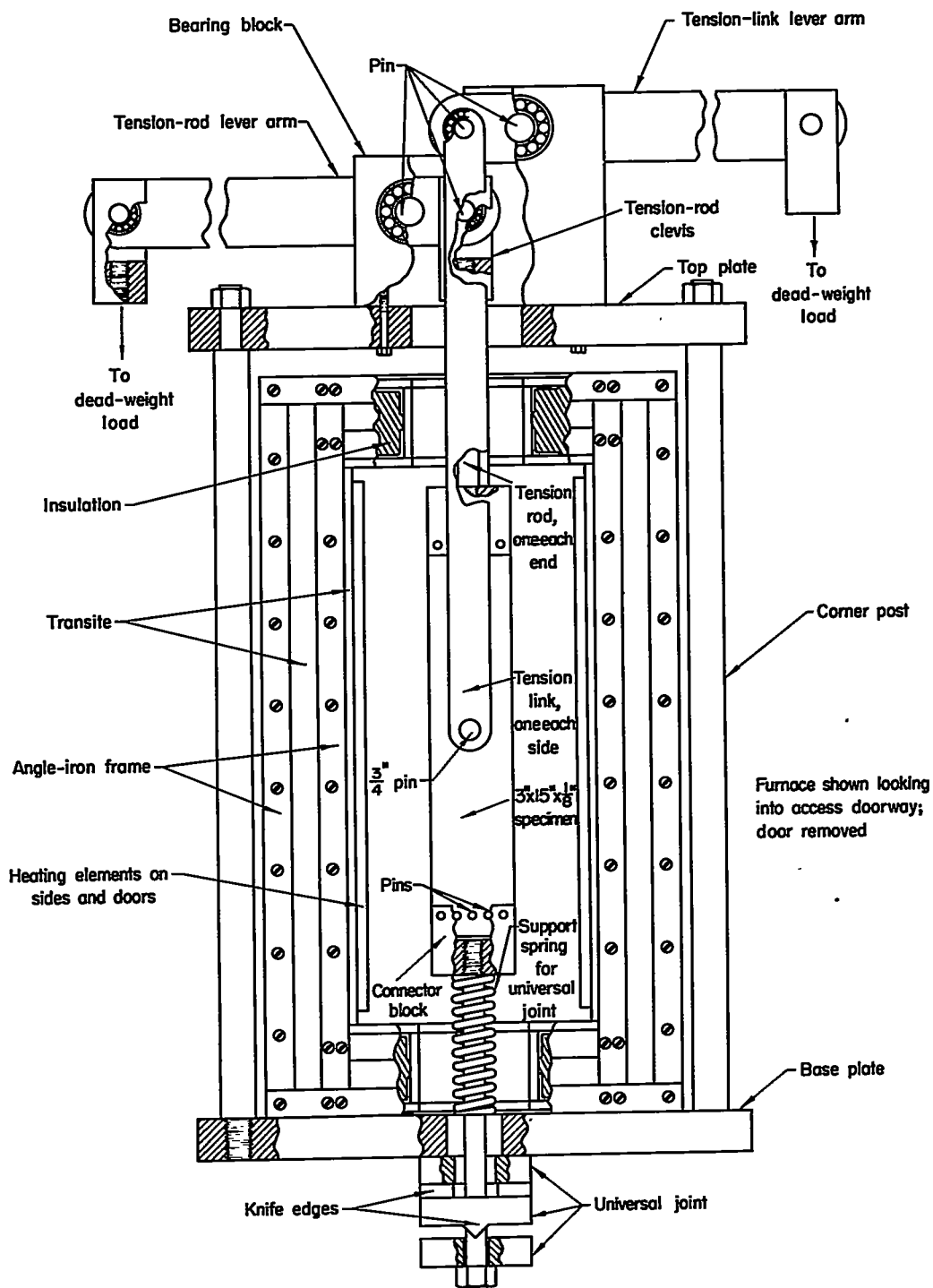


Figure 3.- Loading-frame unit. Furnace shown looking into access doorway; door removed.

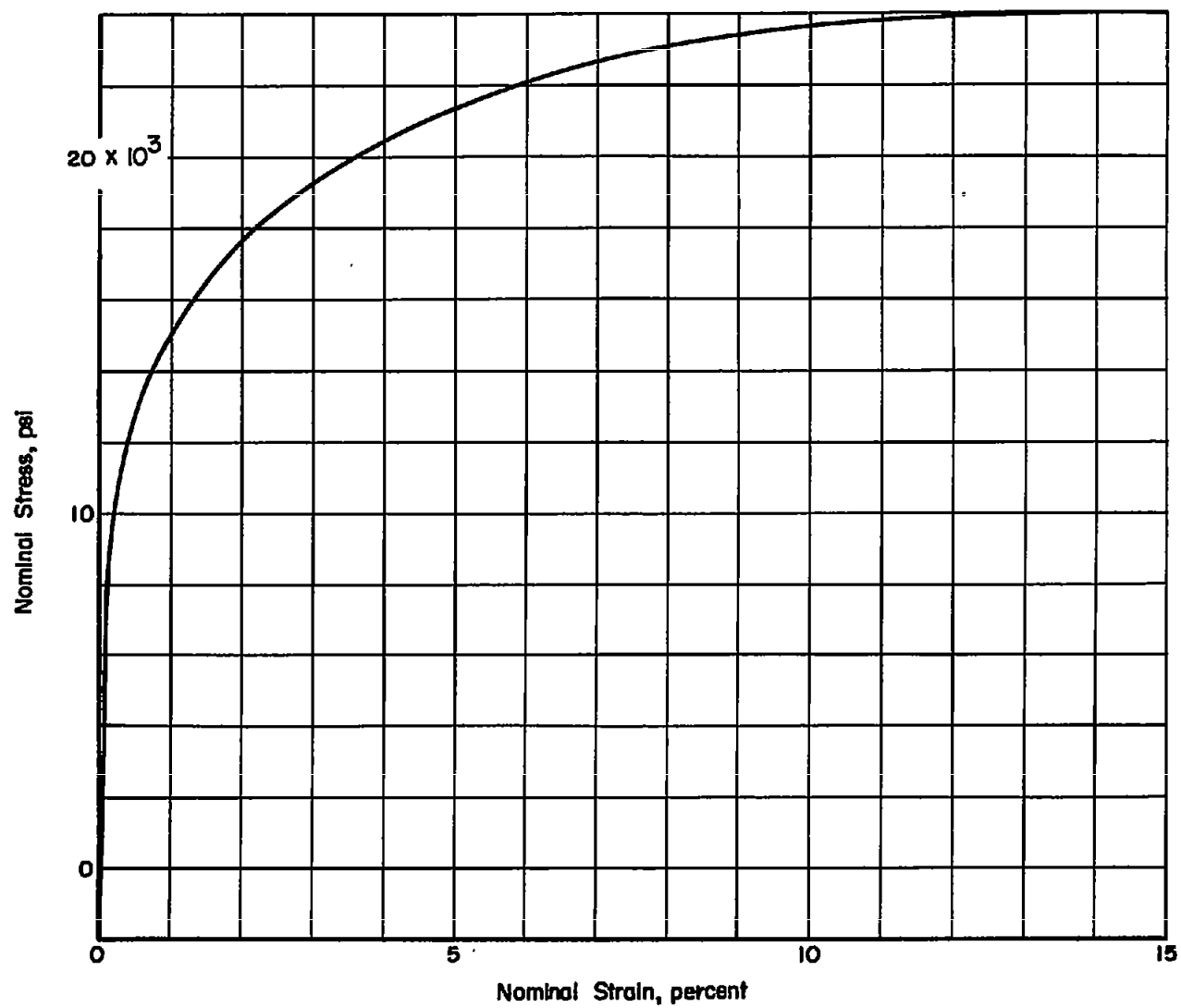


Figure 4.- Stress-strain diagram for 2024-O aluminum alloy at 400° F.

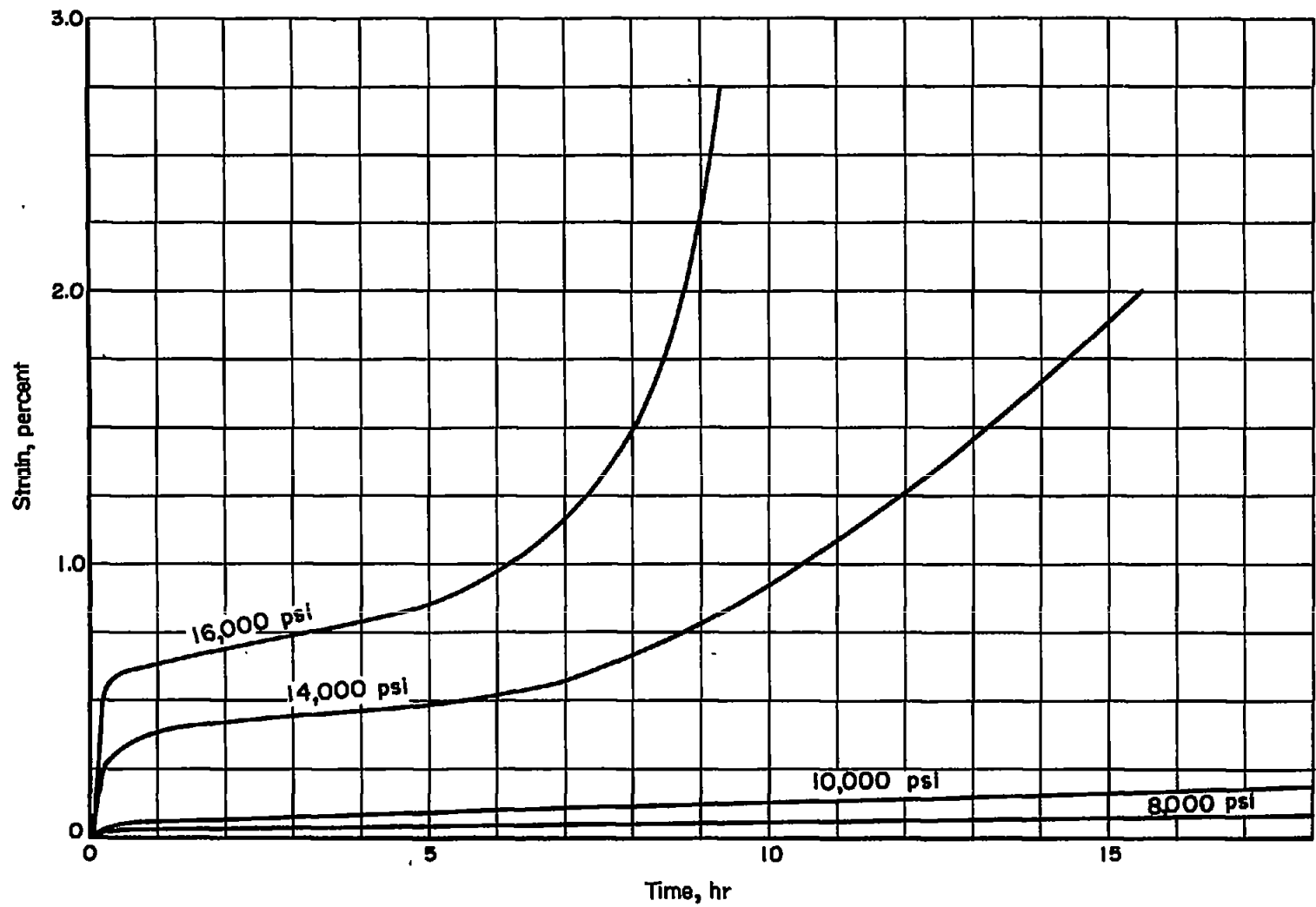


Figure 5.- Creep curves for 2024-O aluminum alloy at 400° F.

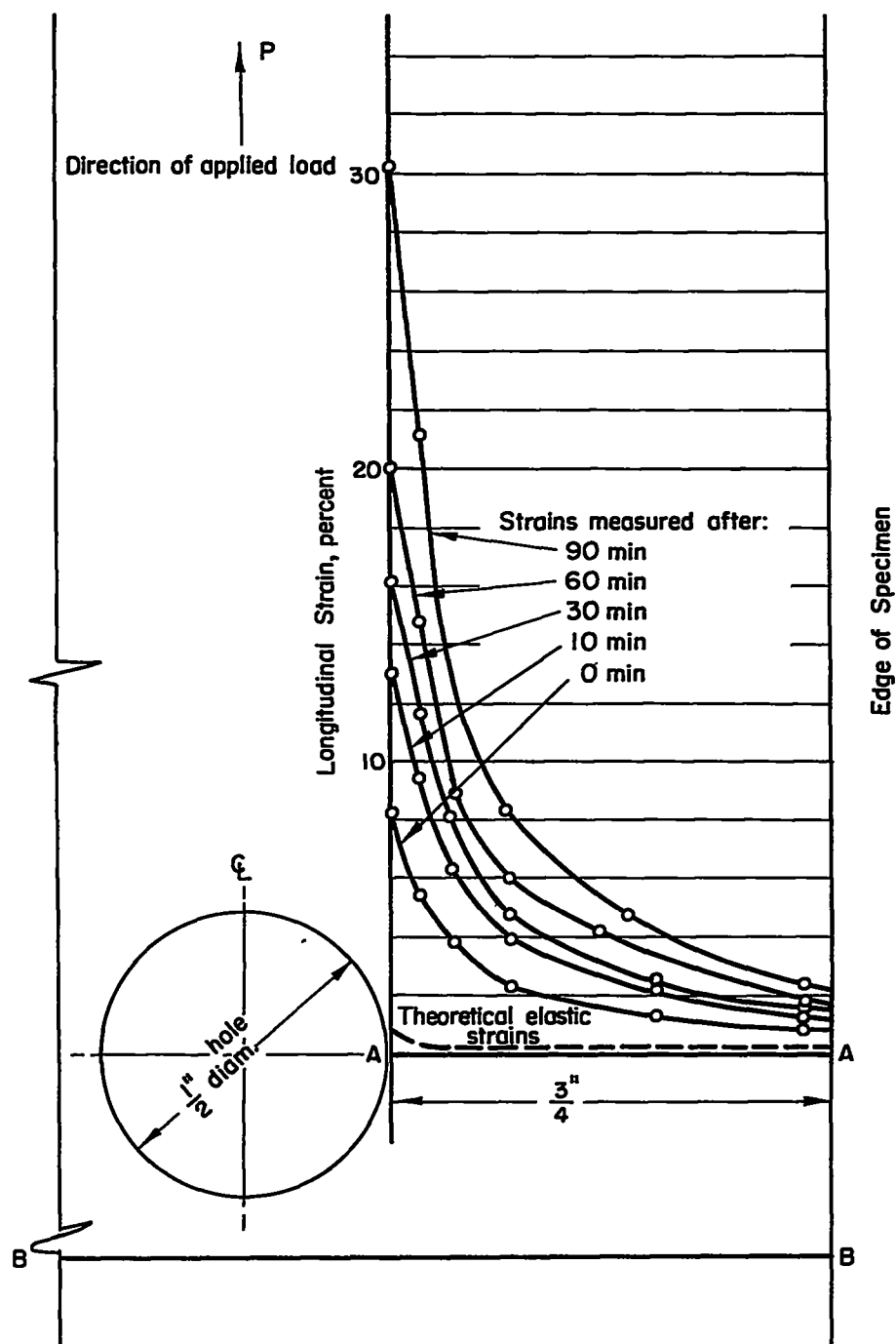


Figure 6.- Creep strains in plate subjected to tension. Test temperature, 400°F ; P , 3,500 pounds; average stress across A-A, 18,700 psi; average stress across B-B, 14,000 psi.

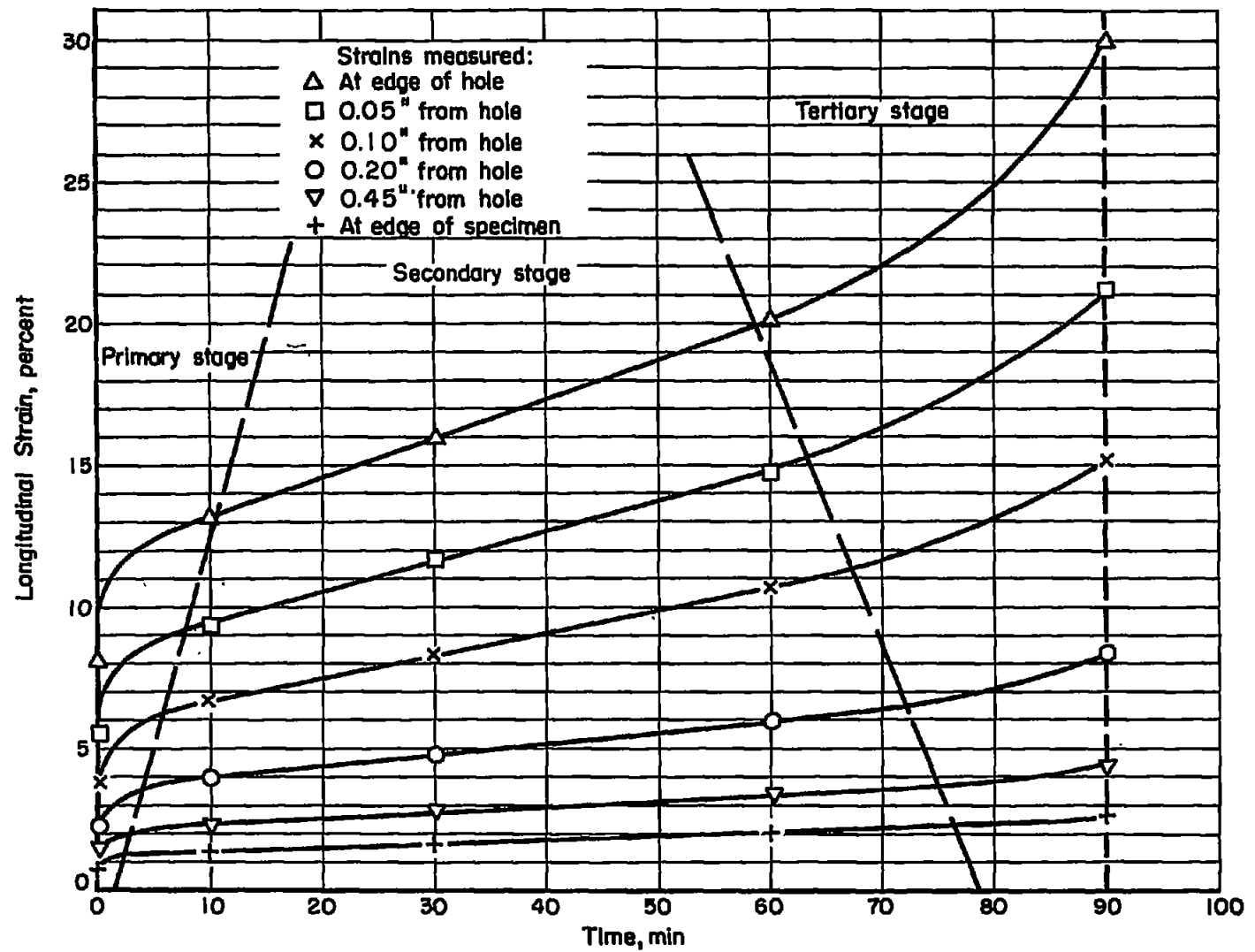


Figure 7.- Strain histories of fibers adjacent to hole for tensile loading.

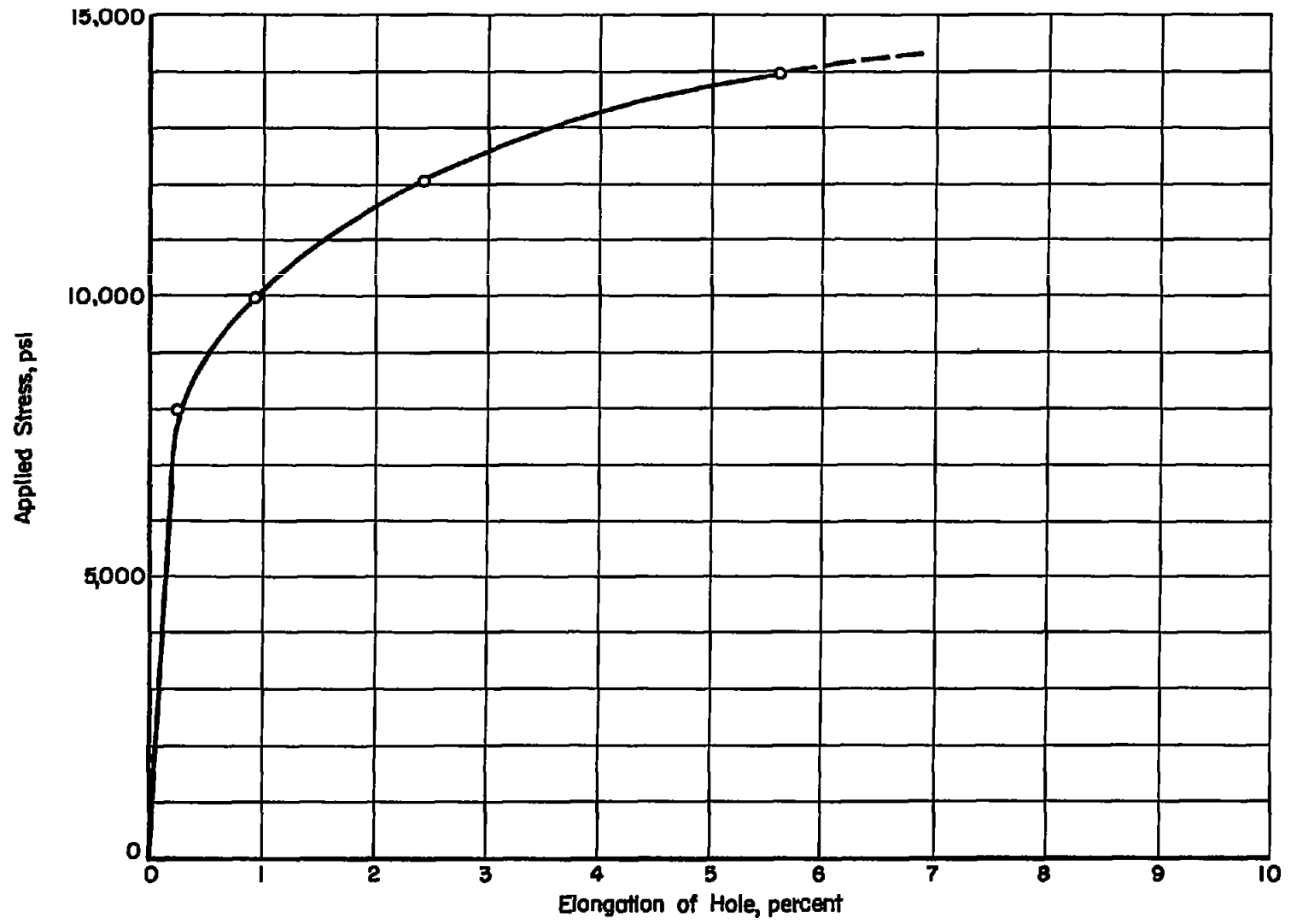


Figure 8.- Plastic elongation of hole in plate subjected to tension.

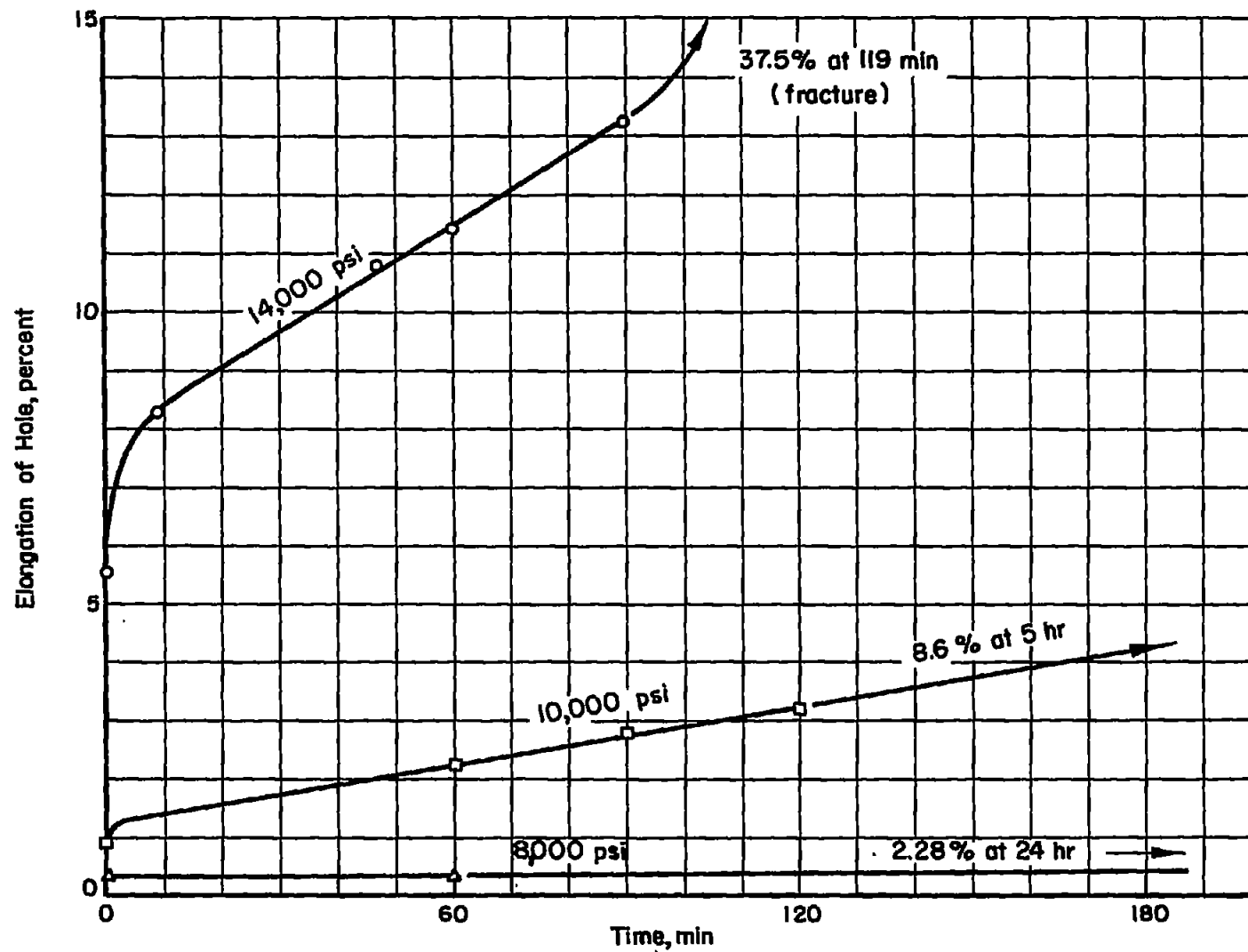


Figure 9.- Creep elongation of a hole in plate subjected to tension.

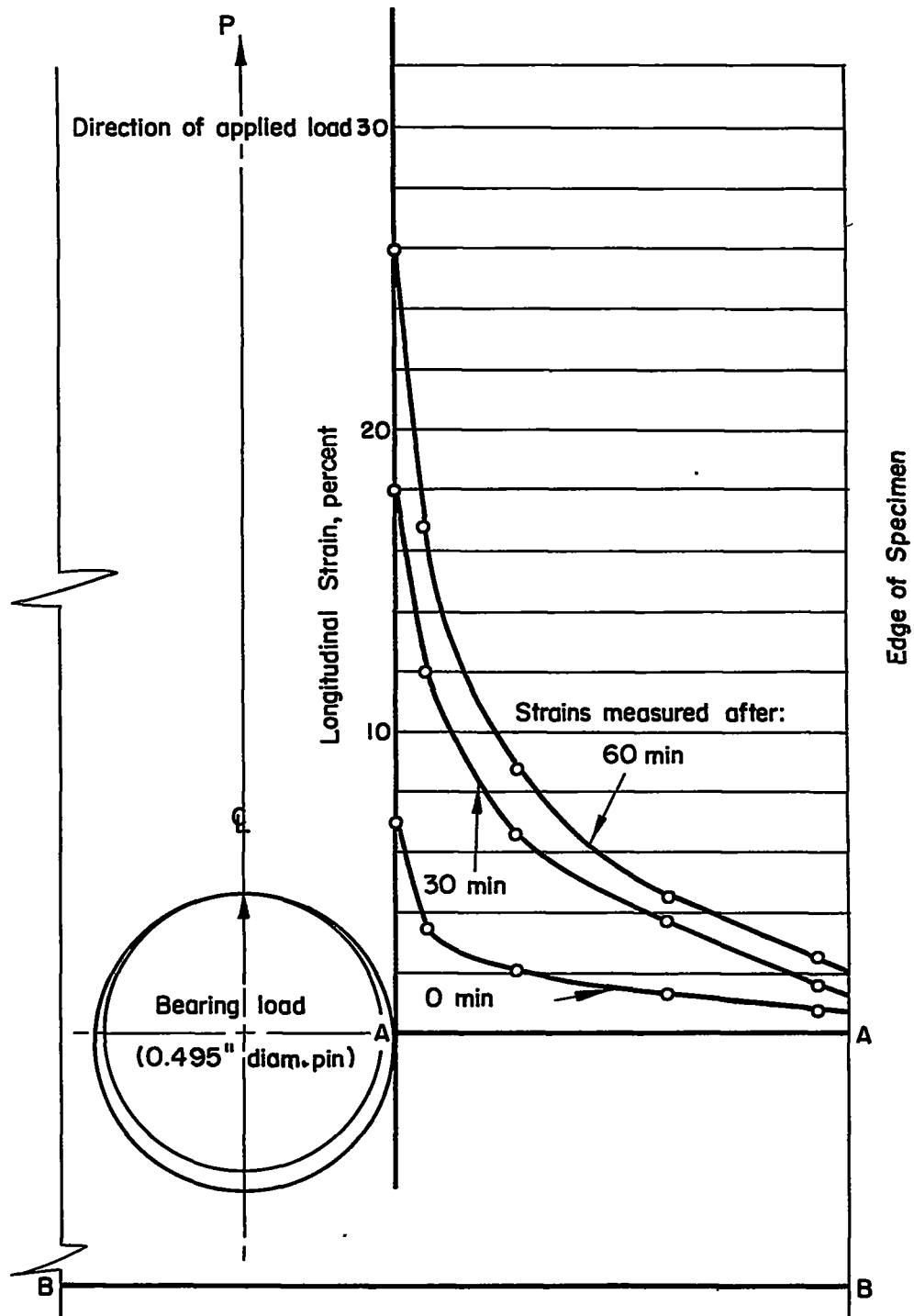


Figure 10.- Creep strains in plate subjected to tension and bearing.
 Test temperature, 400° F; bearing load, 1,750 pounds; P, 1,750 pounds;
 average stress across A-A, 18,700 psi; average stress across B-B,
 14,000 psi.

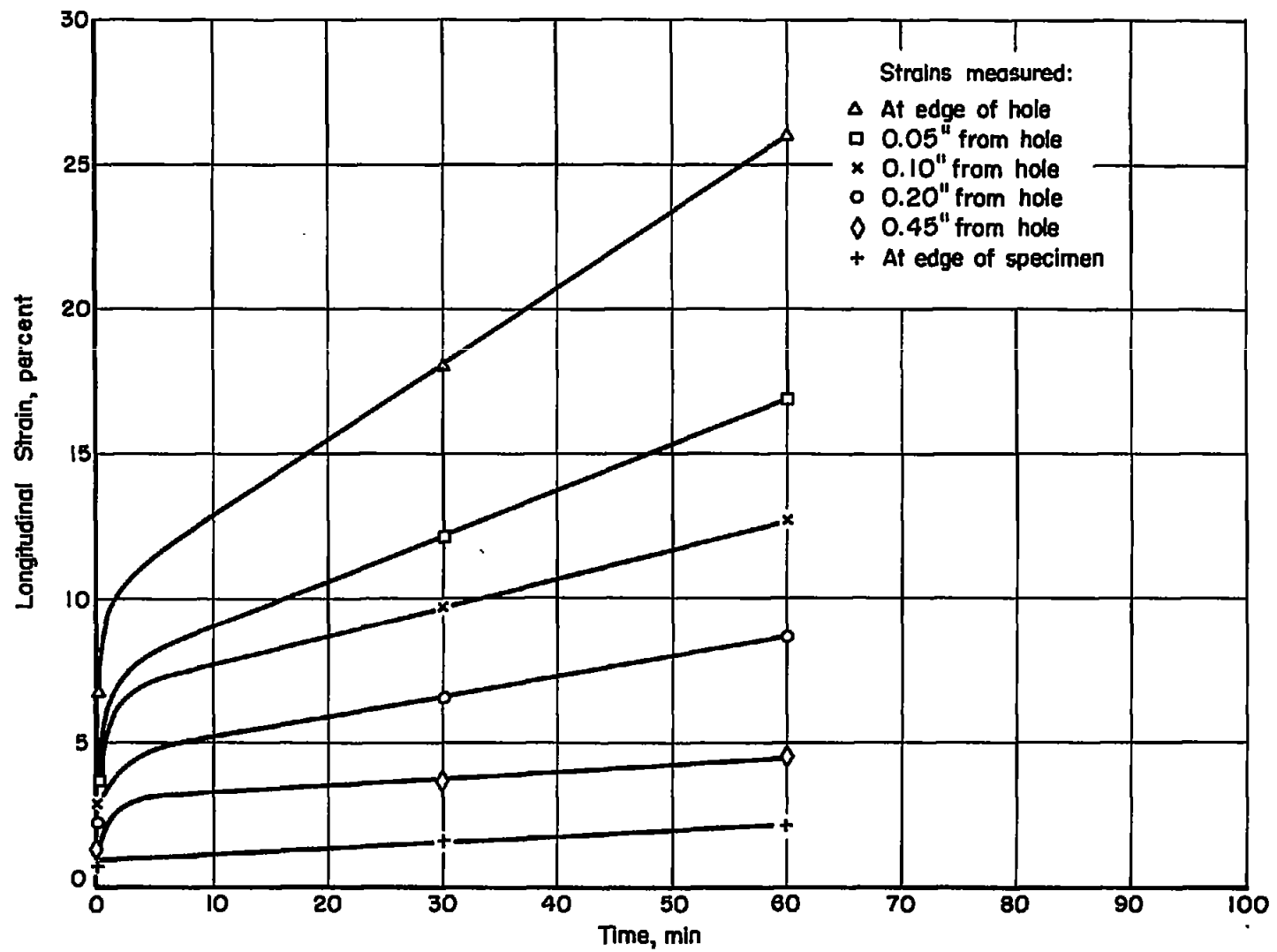


Figure 11.- Strain histories of fibers adjacent to hole for combined loading.

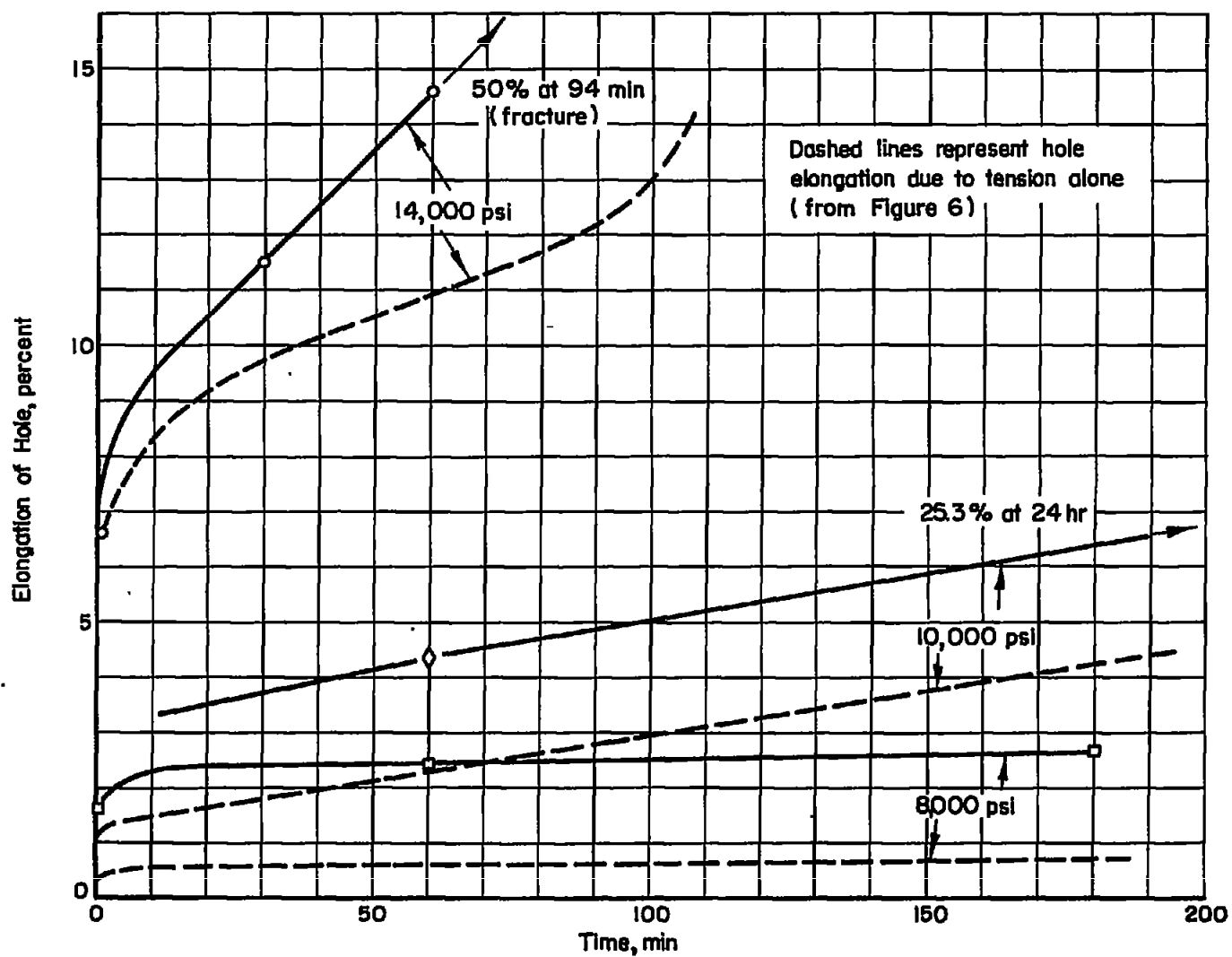


Figure 12.- Effect of combined loading on creep elongation of hole in plate.